

Image Reconstruction from Highly Undersampled (\mathbf{k}, t)-space Data with Joint Partial Separability and Sparsity Constraints

B. Zhao¹, J. Haldar¹, A. Christodoulou¹, and Z-P. Liang¹

¹Electrical and Computer Engineering, University of Illinois at Urbana-Champaign, Urbana, IL, United States

INTRODUCTION

MRI is a relatively slow imaging technique, and the quest for higher imaging speeds has been a major driving force for MRI research since the beginning of the field, resulting in a number of fast imaging methods. Recently, sparse sampling theory has offered another exciting opportunity to further accelerate MRI data acquisition. Two different mathematical approaches to achieving sub-Nyquist sampling are based on the theory of compressed sensing (CS) [1][2] and the theory of partially separable functions [3]. We have developed a novel method for image reconstruction from highly undersampled (\mathbf{k}, t)-space data using constraints from both approaches, achieving better performance than if only one set of constraints had been applied [4].

METHODS

The image reconstruction problem common to most dynamic MRI applications can be formulated as: determine an unknown image function $\rho(\mathbf{r}, t)$ from measurements given by $s(\mathbf{k}, t) = \int \rho(\mathbf{r}, t) e^{-i2\pi \mathbf{k} \cdot \mathbf{r}} d\mathbf{r}$. Here, we assume that (\mathbf{k}, t)-space is highly undersampled so that any direct reconstruction of $\rho(\mathbf{r}, t)$ method will contain significant aliasing artifacts unless additional constraints (beyond bandlimitedness) are invoked. In this work, we propose to use joint partial separability (PS) and sparsity constraints. The PS model assumes $\rho(\mathbf{r}, t) = \sum_{\ell=1}^L g_{\ell}(\mathbf{r}) h_{\ell}(t)$, while the CS model assumes transform sparsity of $\rho(\mathbf{r}, t)$ (e.g. sparsity in the (\mathbf{r}, f)-domain). The effectiveness of the sparsity constraint is dependent on some "randomness" or "incoherence" in data acquisition, while the partial separability constraint is significantly more flexible. Thus data acquisition can be designed to suit both constraints together without any trade-off. In practice, it is convenient to use a strategy which samples a certain region of \mathbf{k} -space densely in time to encode high temporal resolution information and samples the rest of \mathbf{k} -space sparsely to encode high spatial resolution information. Imposing joint partial separability and spatial-spectral sparsity, the image reconstruction can be formulated as [4]

$$\hat{\rho} = \arg \min_{\rho(\mathbf{r}, t) \in \underbrace{\left\{ \sum_{\ell=1}^L g_{\ell}(\mathbf{r}) h_{\ell}(t) \right\}}_{\text{partial separability}}} \underbrace{\| \mathbf{d} - \mathbf{E}\rho \|_{\ell_2}^2}_{\text{data fidelity}} + \underbrace{\lambda \| \Phi \rho \|_{\ell_1}}_{\text{sparsity}}.$$

Note that in the above formulation, $\| \Phi \rho \|_{\ell_1}$ is a measure of the spatial-spectral sparsity of ρ through the ℓ_1 norm, where Φ maps ρ from (\mathbf{r}, t)-domain to the (\mathbf{r}, f)-domain, and \mathbf{E} is the imaging operator. An image reconstruction algorithm based on half-quadratic regularization and continuation is used to solve the above convex optimization problem with global convergence guarantees. The proposed approach has several key features: 1) It absorbs the advantages of both sparsity and partial separability constraints into a single formulation. 2) The two constraints play complementary roles to each other: when the PS model order is high (e.g., 32) or the number of measurements is low, the sparsity constraint serves as an effective regularizer. On the other hand, the partial separability constraint exploits the spatiotemporal correlation of dynamic MR image sequences, helping to remove temporal blurring and recapture subtle image features which are lost when using sparsity alone. 3) We have observed much better reconstruction performance by using explicit partial separability with sparsity constraint than using implicit partial separability (nuclear norm) with a sparsity constraint [5].

RESULTS

We evaluate the performance of the proposed method by a real-time cardiac imaging example. A human cardiac MR numerical phantom was used to simulate a cardiovascular MR experiment on a free-breathing human patient with cardiac arrhythmia. This phantom was created from real human cardiac MR data using retrospective ECG- and respiratory-gating. A time sequence of images representing a single cardiac cycle was reconstructed and temporally interpolated. This image sequence was extended periodically and then time-warped to simulate cardiac arrhythmia. The image sequence was then spatially deformed to generate variable-rate respiratory motion using a thin-plate spline model. In Fig. 1, we compare reconstructions using sparsity alone and partial separability alone against the proposed method using joint constraints. From the reconstructed snapshot images in the first column of Fig. 1, it is easy to see that the proposed method reconstructs cardiac images with higher spatial resolution, especially in the region of the myocardium and blood pools. In contrast, images reconstructed only using a single constraint suffer from much more blurring and artifacts. The second column of Fig. 1 illustrates the temporal evolution of each reconstruction over a vertical line passing through the left ventricle. The temporal characteristics of cardiac motion are more faithfully captured by the proposed method than by the other two methods.

CONCLUSION

A novel image reconstruction method is proposed for using joint partial separability and sparsity constraints for image reconstruction from highly undersampled data. This method should prove useful for many different dynamic imaging applications.

REFERENCES

- [1] Lustig M, *MRM* 2007. pp. 1182-1195. [2] Jung H, *MRM* 2009. pp. 103-116. [3] Liang Z-P, *IEEE-ISBI* 2007. pp. 988-991. [4] Zhao B, *IEEE-EMBS* 2010. pp. 3390-3393. [5] Goud S., *IEEE-ISBI* 2010. pp. 988-991.

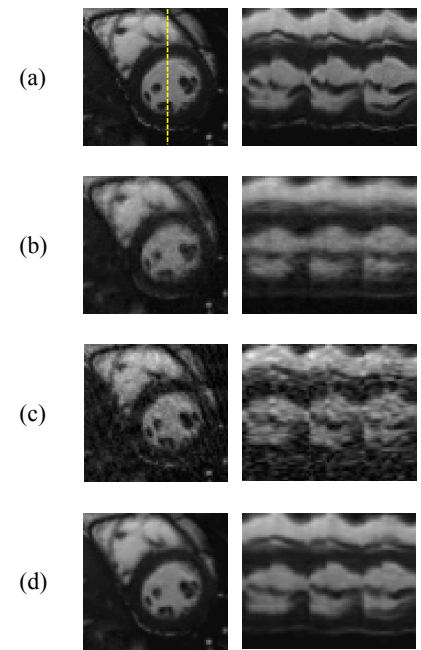


Fig 1. The first column depicts one cardiac phase of the gold standard and reconstructed image sequences. The second column shows the temporal characteristics of a line passing through the left ventricle (visible in the top left image) for the same sequences. The sequences are (a) the gold standard, (b) the reconstruction using CS, (c) the reconstruction using PS, and (d) the reconstruction using joint PS and CS constraints